HoTPiG: A Novel Geometrical Feature for Vessel Morphometry and Its Application to Cerebral Aneurysm Detection

Shouhei Hanaoka[1,2], Yukihiro Nomura[3], Mitsutaka Nemoto[3], Soichiro Miki[3], Takeharu Yoshikawa[3], Naoto Hayashi[3], Kuni Ohtomo[1,3], Yoshitaka Masutani[4], and Akinobu Shimizu[2]

[1] Department of Radiology, The University of Tokyo Hospital, 7-3-1 Hongo, Bunkyo-ku, Tokyo, Japan
[2] Tokyo University of Agriculture and Technology, 2-24-16 Nakamachi, Koganei, Tokyo, Japan
[3] Department of Computational Diagnostic Radiology and Preventive Medicine, The University of Tokyo Hospital, 7-3-1 Hongo, Bunkyo-ku, Tokyo, Japan
[4] Department of Intelligent Systems, Graduate School of Information Sciences, Hiroshima City University, 3-4-1 Otsuka-higashi, Asaminami-ku, Hiroshima, Japan
hanaoka-tky@umin.ac.jp

Abstract. A novel feature set for medical image analysis, named HoTPiG (Histogram of Triangular Paths in Graph), is presented. The feature set is designed to detect morphologically abnormal lesions in branching tree-like structures such as vessels. Given a graph structure extracted from a binarized volume, the proposed feature extraction algorithm can effectively encode both the morphological characteristics and the local branching pattern of the structure around each graph node (e.g., each voxel in the vessel). The features are derived from a 3-D histogram whose bins represent a triplet of shortest path distances between the target node and all possible node pairs near the target node. The extracted feature set is a vector with a fixed length and is readily applicable to state-of-the-art machine learning methods. Furthermore, since our method can handle vessel-like structures without thinning or centerline extraction processes, it is free from the "short-hair" problem and local features of vessels such as caliper changes and bumps are also encoded as a whole. Using the proposed feature set, a cerebral aneurysm detection application for clinical magnetic resonance angiography (MRA) images was implemented. In an evaluation with 300 datasets, the sensitivities of aneurysm detection were 81.8% and 89.2% when the numbers of false positives were 3 and 10 per case, respectively, thus validating the effectiveness of the proposed feature set.

Keywords: graph feature, computer-assisted detection, MR arteriography, cerebral aneurysm, support vector machine.

1 Introduction

A branching treelike structure is one of the major types of structure in the human body. For example, a wide variety of vessels (blood vessels, bronchi, bile ducts, etc.)

N. Navab et al. (Eds.): MICCAI 2015, Part II, LNCS 9350, pp. 103–110, 2015.
DOI: 10.1007/978-3-319-24571-3_13

have a treelike structure. Quite a large number of diseases affect these vascular structures and cause pathological shape changes including narrowing, occlusion, and dilation. Vascular diseases, including cerebral infarction and coronary occlusive disease, are one of the major causes of death in advanced nations. Since precise evaluation of the shape of vessels is essential in diagnosing these diseases, computer-assisted detection/diagnosis (CAD) of these treelike structures is required.

Among the vascular diseases, cerebral aneurysm has been one of the targets of CAD applications [1-3]. Although unruptured cerebral aneurysms are generally asymptomatic, they rupture in approximately 1% of patients per year, leading to high rates of mortality and disability [2]. This is why the early detection of cerebral aneurysms is needed. In clinical practice, noninvasive magnetic resonance arteriography (MRA) examination is most frequently used for screening, in which diagnostic radiologists search for abnormal structures (i.e., saccular protuberances and fusiform dilation). However, it is known that a normal arterial system may include pseudo-lesions such as infundibular dilatations. CAD applications for detecting cerebral aneurysm also have to distinguish abnormal aneurysmal structures from normal ones, including branching sites of small cerebral arteries and tightly curving carotid siphons.

In previous studies, two approaches to searching for aneurysms have generally been used: (1) voxel-by-voxel evaluation using Hessian matrix-derived features, and (2) three-dimensional (3-D) thinning of a presegmented arterial region and branching pattern analysis. In the first approach, a Hessian-based filter emphasizes spherical structures with various sizes. For example, Arimura et al. [3] used a dot enhancement filter that outputs a high value when all three eigenvalues of the Hessian matrix have large negative values. Nomura et al. [2] used a similarity index that can distinguish spherelike aneurisms from ridgelike vessels. Although their approach usually works well, the detected candidates inevitably include a large number of false positives, especially at vessel bifurcations. Therefore, subsequent processes to eliminate false positives are required, greatly affecting the overall performance.

The other approach is to find an abnormal arterial branching pattern from the graph structure of an extracted artery. After segmentation of the artery voxels, a 3-D thinning algorithm is applied to extract the centerlines. Then the centerlines are analyzed to find any suspicious points, such as end points of centerlines [4], short branches, or points with a locally maximal vascular radius [1]. In contrast to the curvature approach, the centerline approach can utilize branching pattern information to discriminate aneurysms from bifurcations. On the other hand, the 3-D thinning process has the "short hair" problem, i.e., a large number of false short branches where the arterial wall has small "lumps." Therefore, a postprocess to remove [5] or classify [1, 3] short hairs is indispensable. Another problem is how to represent local morphological and topological changes in the graph in the context of machine learning. A large number of studies on the analysis of whole graph structures have been conducted in which the graph structure is embedded into a vector field (graph embedding) or evaluated by kernel methods (graph kernel) [6].

In this study, we propose a novel feature set named HoTPiG (Histogram of Triangular Paths in Graph). It is defined at each node in a given graph based on a 3-D histogram of shortest path distances between the node of interest and each of its

neighboring node pairs. The feature vector efficiently encodes the local graph network pattern around the node. The graph structure can be determined directly from a binary label volume. Since the thickness of the vessel is naturally encoded without any centerline extraction process, the "short hair" problem caused by the thinning algorithm does not occur. Furthermore, the proposed feature is essentially robust to nonrigid deformations under the assumption that the graph structure extracted from the original image is not significantly changed by the deformation. The proposed feature set is sufficiently effective for aneurysms in MRA images to be accurately classified by a support vector machine (SVM) without any complicated pre- or postprocesses. The contributions of this study are as follows: (1) A novel vector representation of a local graph structure for detecting abnormalities is presented, (2) a CAD application for detecting aneurysms in MRA images is implemented using the proposed graph feature and a state-of-the-art SVM classifier with explicit feature mapping, and (3) the usefulness of the proposed method is experimentally validated using a large dataset with 300 clinical MRA images, and high performance comparable to that of other state-of-the-art methods is demonstrated.

2 HoTPiG

The proposed HoTPiG feature is defined for any arbitrary undirected graph based on bin counts of a 3-D histogram of shortest path lengths (Fig. 1). One feature vector is determined for each node in the graph and can be readily used to classify the corresponding node as positive (e.g., aneurysm) or negative. The 3-D histogram accumulates counts of each triplet of distances between the target node and its two neighbor nodes as well as between the two neighbor nodes.

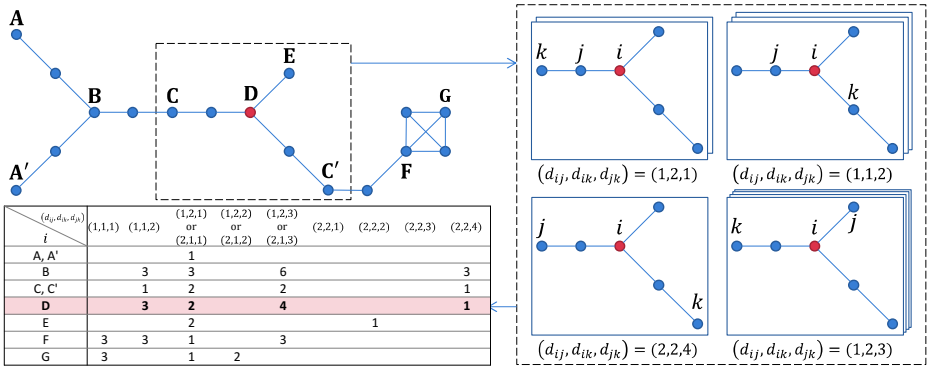

i \ (d_{ij}, d_{ik}, d_{jk})	(1,1,1)	(1,1,2)	(1,2,1) or (2,1,1)	(1,2,2) or (2,1,2)	(1,2,3) or (2,1,3)	(2,2,1)	(2,2,2)	(2,2,3)	(2,2,4)
A, A'			1						
B		3	3		6				3
C, C'		1	2		2				1
D		**3**	**2**		**4**				**1**
E			2				1		
F	3	3	1		3				
G	3		1	2					

Fig. 1. Example of calculation of HoTPiG features (with $d_{max} = 2$).

Suppose that the graph includes $|U|$ nodes, and each node in the graph has an integer index $l \in \mathrm{U} = \{1,2,3,\ldots,|U|\}$. Also suppose that the feature vector of node i is to be calculated. First, the shortest path distances from i to all other nodes are calculated (by a breadth first search). Here, the shortest path distance is the number

of steps (edges) along the shortest path between the pair of nodes. Let the distance between nodes a and b be $dist(a,b)$. We define the *neighborhood* of i, N_i, as the set of nodes whose distances from i are no more than a predefined integer d_{max}. That means $N_i = \{l \in U | 0 < dist(i,l) \leq d_{max}\}$.

Then, for any triplet of distances (d_{ij}, d_{ik}, d_{jk}), the value of the 3-D histogram $H_i(d_{ij}, d_{ik}, d_{jk})$ is defined as the number of node pairs (j,k) that satisfy the following conditions

$$j \in N_i, k \in N_i, dist(i,j) = d_{ij}, dist(i,k) = d_{ik}, dist(j,k) = d_{jk}. \quad (1)$$

In practice, the two bins (d_{ij}, d_{ik}, d_{jk}) and (d_{ik}, d_{ij}, d_{jk}) are simply those with neighbor nodes j and k swapped. Thus, these two bins are considered to be the same and only one count is incremented for such pairs of distance triplets.

The counts of bins in histogram H_i are used as the feature vector of node i. As shown in Fig. 1, the feature vector tends to vary widely among different nodes and is sensitive to topological changes in the local graph structure. Note that the extent of the locality can be controlled via the parameter d_{max}.

The calculation cost for the proposed method is estimated as follows. The breadth-first search algorithm can calculate all the shortest path distances by performing $O(|U| \cdot E(|N_i|))$ calculations, where $E(|N_i|)$ is the mean size of the neighborhoods. On the other hand, the histogram counting requires $O(|U| \cdot E(|N_i|)^2)$ count increment calculations. Therefore, most of the calculation cost is for histogram counting.

3 Computer-Assisted Detection of Aneurysms

As an application of the proposed HoTPiG feature, we have developed CAD software for aneurysm detection in MRA images. The proposed CAD application is composed of four steps: (1) extraction of the binary label volume of arteries from MRA images, (2) calculation of graph structure features, (3) voxel-based classification by SVM, and (4) a thresholding and labeling process.

3.1 Artery Region Extraction and HoTPiG Feature Calculation

Firstly, the artery region is extracted by a conventional region growing method. The average $\bar{I}$ and standard deviation σ_I of the brain region are estimated by sampling voxel values from a predefined mid-central subregion, that is, a horizontal rectangular plane with half the width and height placed at the center of the volume. Then, the initial artery region is extracted by region growing, where the seed threshold and growing threshold are $> \bar{I} + 3\sigma_I$ and $> \bar{I} + 2.5\sigma_I$, respectively.

After the artery region is extracted, an undirected graph is composed. We choose a simple graph structure whose nodes are all foreground (i.e., intra-arterial) voxels, and the edges connect all 18-neighbor voxel pairs (Fig. 2). Here, an 18-neighborhood is chosen because it is more similar to the Euclidean distance than 6- and 26-neighborhoods.

Using this graph, the HoTPiG feature is calculated at each foreground voxel. The maximum distance used is $d_{max} = 11$, considering the balance between the performance and the calculation cost. Two modifications are applied to the method described in Section 2. Firstly, a 1-D histogram with $d_{max} = 11$ bins whose distances are $\{1, 2, 3, \ldots, 11\}$ may be too sparse when it is used as part of a 3-D histogram. To cope with this, some distances are grouped into one bin and only six bins $\{1, 2, 3, [4, 5], [6, 7], [8, 11]\}$ are used. These bins are determined so that their upper bounds are the geometric series $1.5^{\mathrm{n}}, \mathrm{n} = 1,2,3,4,5,6$. Applying this bin set to each of three distances (d_{ij}, d_{ik}, d_{jk}), the entire 3-D histogram has $6 \cdot_6 \mathrm{C}_2 = 126$ bins. However, some bins never have a count because the corresponding distance triplet does not satisfy the triangle inequality. After removing such bins, a total of 85 bins are included in the 3-D histogram in this study.

Additionally, a multidimensional approach is added to analyze gross vascular structures. After downsampling the artery binary volume to half and a quarter of its original size, the graph structure features are extracted in the same manner. After feature extraction, each feature is upsampled by nearest neighbor interpolation and all the features of the three scales are merged voxel by voxel. Therefore, a total of $85 \times 3 = 255$ features are calculated for each voxel.

Prior to the classification process, each feature is normalized by dividing by the standard deviation estimated from training datasets.

3.2 Voxel-Based Classification by SVM

Using the extracted features, each voxel is classified as positive (aneurysm) or negative (normal artery) by a an SVM classifier [7]. The exponential-χ^2 kernel $K(\mathbf{x}, \mathbf{y}) = \exp\left(-\frac{1}{2\sigma^2} \cdot \frac{1}{2}\sum_l \frac{(x_l - y_l)^2}{x_l + y_l}\right)$ [8], which is designed specifically for histogram comparison, is used in this study. The classifier is trained using manually inputted aneurysm voxels in the training datasets as positive samples and other arterial voxels as negative samples. Here, one of the difficulties is the huge number ($> 10^8$) of training samples, because one MRA volume has approximately 10^6 artery voxels. It is known that the computational cost of kernel SVM is of order $O(dM^2) \sim O(dM^3)$, where d and M are the data dimensionality and number of samples, respectively. To solve this problem, we utilized a feature map of the exponential-χ^2 kernel [8] to reduce the original problem to a linear SVM whose computational cost is $O(dM)$. The feature map is a function that *explicitly* maps the original feature vector of each sample to a higher-dimensional space, in contrast to the conventional kernel method, in which a vector is *implicitly* mapped to a higher-dimensional space. Using this feature map and the random reduction of negative samples (to 3% of the original number), the training task was calculated in approximately 20 min for 2×10^8 original samples.

In addition to the classifier with the HoTPiG feature set only, another classifier is also trained by adding two sets of Hessian-derived features (the dot enhancement filter [3] and shape index [2]) to evaluate the cooperativity of both types of features. The two Hessian-derived features are calculated with six different scales; thus, a total of 12 features are added to the HoTPiG features.

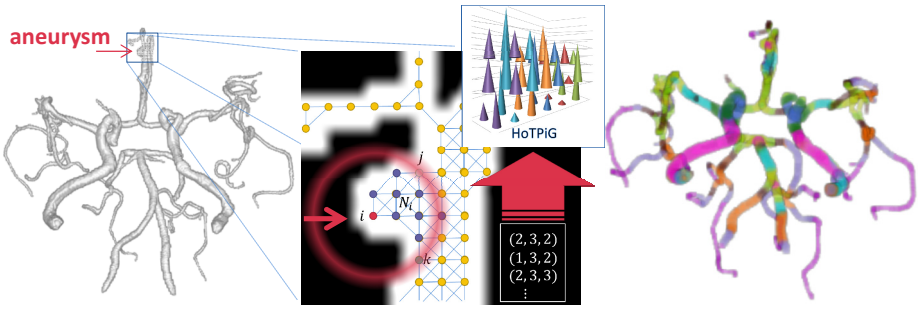

Fig. 2. (Left) Example of cerebral arteries in a volume. (Middle) HoTPiG feature calculation for a voxel in an aneurysm. (Right) Result of voxelwise clustering of HoTPiG features into 20 clusters (displayed by their colors) by a k-means method. Note that the vessel thickness and branching pattern can be clearly distinguished. Furthermore, the mirror symmetry of the clustering result implies its robustness against local deformations and sensitivity to caliper changes.

In this study, the parameters of feature mapping are set to $m = 5000$, $n = 2$, and $L = 0.6$, referring to [8]. The parameters of the kernel σ and the linear SVM C are experimentally optimized (as described later in the next section).

Using the output values of the SVM, candidate aneurysm lesions and their lesionwise likelihoods are determined as follows. Firstly, the SVM outputs are thresholded by zero and all nonpositive voxels are discarded. Then, the positive voxels are labeled by connected component analysis and all connected components are outputted as candidate lesions. The likelihood of each lesion is determined as the maximal value of SVM-derived likelihoods of the voxels in the lesion. The representative point of each lesion is defined as this maximal value point.

4 Experimental Results

This study was approved by the ethical review board of our institution. A total of 300 time-of-flight cerebral MRA volumes with 333 aneurysms were used in the experiment. The voxel size was 0.469×0.469×0.6 mm. Two board-certified radiologists diagnosed all images and manually inputted aneurysm regions.

The proposed method was evaluated using 3-fold cross-validation. Before the actual training, a hyperparameter optimization was performed in each fold using another nested 3-fold cross validation. The optimal values of the two parameters σ and C were searched for from the search space $\sigma \in \{20,30,40\}$ and $C \in \{10,20,30\}$ by performing a grid search. After optimization, the actual training was performed using all training datasets. The calculation of HoTPiG features took approximately 3 min per case using a workstation with 2 ×6 core Intel Xeon processers and 72 GB memory.

The overall performance of the method was evaluated using the free receiver operating characteristic (FROC) curve. Each outputted lesion was determined as a successful detection if the representative point of the lesion was no more than 3 mm from the center of gravity of the ground truth region.

Figure 3 shows the FROC curves of the proposed method with and without additional Hessian features, as well as the one with Hessian features only. The sensitivities with only HoTPiG features were 76.6% and 86.5% when the numbers of false positives (FPs) were 3 and 10 per case, respectively. When combined with Hessian features, the sensitivities increased to 81.8% and 89.2% for 3 and 10 FPs/case, respectively. Although a strict comparison cannot be made owing to the different datasets used, the sensitivity of 81.8% is superior to that reported by Yang et al. [1], whose detection sensitivity was 80% for 3 FPs/case. On the other hand, Nomura et al. [2] reported sensitivities of 81.5% and 89.5% when the training dataset sizes were 181 and 500 (also for 3 FPs/case), respectively. Since we used 200 datasets to train each SVM, we conclude that the performance of our CAD is comparable to that of Nomura et al. when the dataset size is equal. Note that Nomura et al. did not use any objective criterion (e.g., maximum acceptable error distance) to judge lesions outputted by CAD as true positives or false positives; instead, radiologists subjectively decided whether or not each CAD-outputted lesion corresponded to an aneurysm.

Figure 3 also shows the sensitivity for each aneurysm size (maximized by using 21 FPs/case). Most detection failures occurred when the size of the aneurysms was less than 4 mm. On the other hand, our method failed to detect two large aneurysms whose sizes were 6 mm and 13 mm. This was very likely to have been due to a shortage of large aneurysms (only 19 with sizes $\geq$ 6 mm) in our dataset.

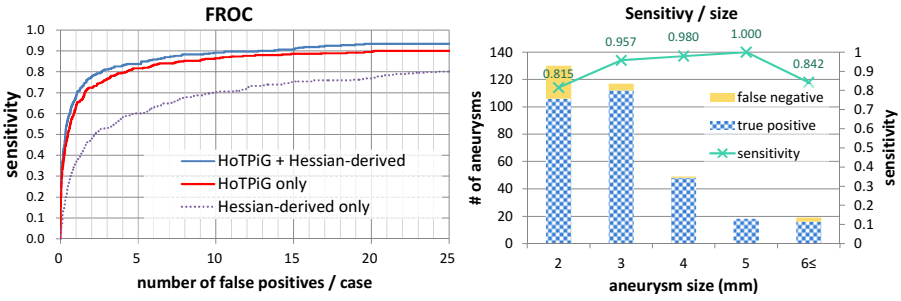

Fig. 3. (Left) FROC curves for the proposed method with and without additional Hessian-derived features. (Right) Sensitivities (with Hessian features) for each aneurysm size.

5 Discussion and Conclusion

Among the various vascular diseases that involve the human body, aneurysms are characterized by their particular protuberant shape. This study was inspired by the fact that many radiologists rely on 3-D reconstructed vascular images to find aneurysms and other diseases in daily image interpretation. This implies that only the shape of the tissue can be sufficient to detect such abnormalities. The HoTPiG feature is designed to evaluate only the shape of the tissue and discard all image intensity information including image gradations and textures. This can be both a disadvantage and an advantage of HoTPiG. On the one hand, it can only utilize a small part of the information provided by the original image. On the other hand, HoTPiG

can reveal image characteristics very different from those collected by most other image features based on image intensity information. Indeed, HoTPiG showed cooperativity with existing Hessian-based features which has a weakness at branching sites of vessels. The effectiveness of HoTPiG shown in this study may also be owing to the robustness of HoTPiG against local deformations. Therefore, we believe that HoTPiG will be a powerful alternative tool for vectorizing shape characteristics of vessel-like organs.

In conclusion, a novel HoTPiG feature set for evaluating vessel-like shapes was presented. It showed high performance for detecting cerebral aneurysms and cooperativity with existing image features. Our future works may include the application of HoTPiG to other applications such as lung nodule detection, in which discrimination between lesions and vascular bifurcations has similar importance.

Acknowledgement. This study is a part of the research project "Multidisciplinary Computational Anatomy", which is financially supported by the grant-in-aid for scientific research on innovative areas MEXT, Japan.

References

1. Yang, X., Blezek, D.J., Cheng, L.T., Ryan, W.J., Kallmes, D.F., Erickson, B.J.: Computer-aided detection of intracranial aneurysms in MR angiography. Journal of Digital Imaging 24, 86–95 (2011)
2. Nomura, Y., Masutani, Y., Miki, S., Nemoto, M., Hanaoka, S., Yoshikawa, T., Hayashi, N., Ohtomo, K.: Performance improvement in computerized detection of cerebral aneurysms by retraining classifier using feedback data collected in routine reading environment. Journal of Biomedical Graphics and Computing 4, 12 (2014)
3. Arimura, H., Katsuragawa, S., Suzuki, K., Li, F., Shiraishi, J., Sone, S., Doi, K.: Computerized scheme for automated detection of lung nodules in low-dose computed tomography images for lung cancer screening 1. Academic Radiology 11, 617–629 (2004)
4. Suniaga, S., Werner, R., Kemmling, A., Groth, M., Fiehler, J., Forkert, N.D.: Computer-aided detection of aneurysms in 3D time-of-flight MRA datasets. In: Wang, F., Shen, D., Yan, P., Suzuki, K. (eds.) MLMI 2012. LNCS, vol. 7588, pp. 63–69. Springer, Heidelberg (2012)
5. Kobashi, S., Kondo, K., Yutaka, H.: Computer-aided diagnosis of intracranial aneurysms in MRA images with case-based reasoning. IEICE Transactions on Information and Systems 89, 340–350 (2006)
6. Suard, F., Guigue, V., Rakotomamonjy, A., Benshrair, A.: Pedestrian detection using stereo-vision and graph kernels. In: Proceedings of the IEEE Intelligent Vehicles Symposium, pp. 267–272. IEEE (2005)
7. Fan, R.-E., Chang, K.-W., Hsieh, C.-J., Wang, X.-R., Lin, C.-J.: LIBLINEAR: A library for large linear classification. The Journal of Machine Learning Research 9, 1871–1874 (2008)
8. Sreekanth, V., Vedaldi, A., Zisserman, A., Jawahar, C.: Generalized RBF feature maps for efficient detection. In: Proceedings of the British Machine Vision Conference (BMVC), Aberystwyth, 31 August - 3 September, pp. 1–11 (2010)